Electronic Supplementary Material (ESI) for Nanoscale.

Selective Switching of Multiple Plexcitons in Colloidal Materials: Directing the Energy Flow at the Nanoscale

Nicola Peruffo,[1] *Gabriel Gil,*[1, †] *Stefano Corni,*[1,2] *Fabrizio Mancin,*[1] *Elisabetta Collini*[1] *

[1] Department of Chemical Sciences. University of Padova, via Marzolo 1, 35131 Padova, Italy
[2] CNR-NANO Institute of Nanoscience, v. Campi 213/a, 41125 Modena, Italy
† present address: Institute of Cybernetics, Mathematics and Physics (ICIMAF), La Habana, Cuba

*elisabetta.collini@unipd.it

Supporting Information

Contents

1. Experimental procedures

1.1 Materials

The 8-trimethylammonium octylthiol capping molecule was synthesized following the procedure described in ref. ([1]). All the solvents and reactants were obtained from Sigma-Aldrich (Merck KGaA, Darmstadt, Germany) and used as received without further purification. The 4,4′,4″,4‴-(Porphine-5,10,15,20-tetrayl) tetrakis(benzenesulfonic acid) was bought by PorphyChem.

1.2 Synthesis and characterization of thiol monolayer protected gold nanoparticles

Citrate capped gold nanoparticles (tA-NPs) were prepared according to a modified version of a literature procedure.[2] Typically, 1.65 mL of sodium citrate (510 mM), 250 μL of silver nitrate (10 mM) and 500 μL of tetrachloroauric acid (253 mM) were added in this precise sequence to 5.6 mL of water, under vigorous stirring. The resulting solution is stirred for 5 min. During this time, the solution changed from the initial yellow color to green. After the incubation time, the solution was quickly added to 117 mL of boiling water and heated under reflux for 1 h, becoming wine-red after a few seconds. The resulting citrate-capped nanoparticles solution was then allowed to cool down to room temperature. Subsequently, 2 mL of the 8-trimethylammonium octylthiol solution (33mM) were added and the solution was allowed to react overnight under stirring. The solution was filtered by a 0.2 μm syringe filter to remove large aggregates and then, to eliminate the citrate impurities, it was washed five times with a 100kDa cutoff filter (Amicon® - Ultra) (previously washed three times with 1:1 EtOH:water).

2. Characterization of citrate capped and thiol capped nanoparticles

TEM analysis was performed with a Jeol 300 PX electron microscope and the collected images were analysed with ImageJ software. Figure S1shows a TEM image relative to a sample of tA-NPs. The average diameter is 11±2 nm (300 measurements). We do not expect that the polydispersity of NPs affects significantly the optical proprieties of the nanohybrids. Indeed, the electronic properties of the plasmon and the curvature radius of the particle do not vary significantly for NPs with diameters in the range 9-14nm.[3]

TGA analysis of a sample of tA-NPs under air atmosphere is shown in Figure S2. Thermogravimetric analysis (TGA) was run on 1 mg nanoparticle samples using a Q5000 IR model TA. The measurement was set to reach 100°C and to keep this temperature for 10’, in order to remove completely the water traces, and then arrive to 1000 °C under a continuous air flow.

The average formula, calculated on the basis of TEM diameter and TGA analysis using a spherical approximation for the gold core and a density of 59 gold atoms per nm^3, is $Au_{30891}(RS)_{2426}$.

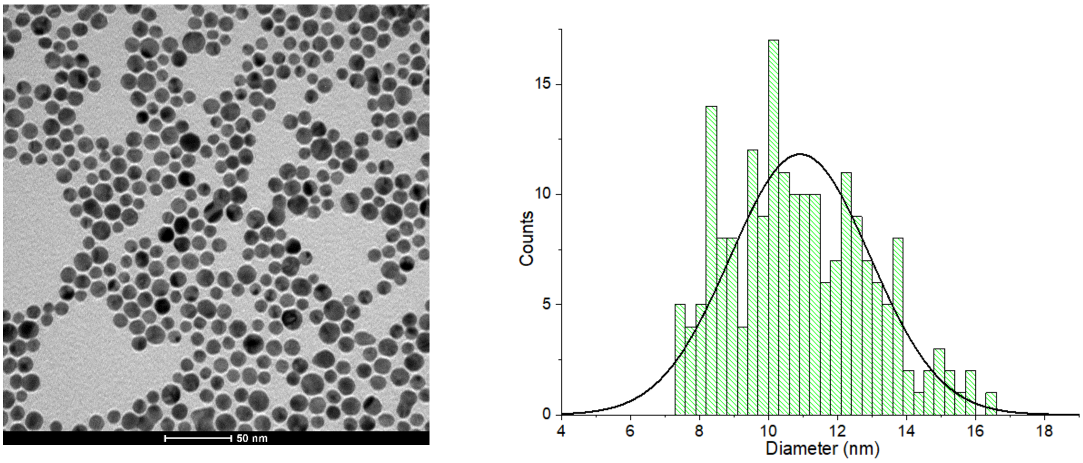

Figure S1: (left) TEM image recorded for a sample of tA-NPs. (right) Size distribution: average diameter = 11 nm (σ=2 nm).

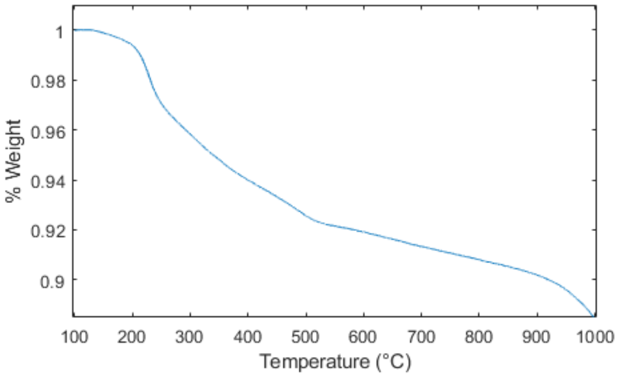

Figure S2: TGA analysis of a sample of tA-NPs under air atmosphere.

NMR analysis (Figure S3) was used to verify the formation of the thiol monolayer, as proved by the broadening of all signals. NMR spectra were recorded using a Bruker AV III 500 spectrometer operating at 500 MHz for 1H. Chemical shifts are reported relatively to the internal standard Me_4Si.

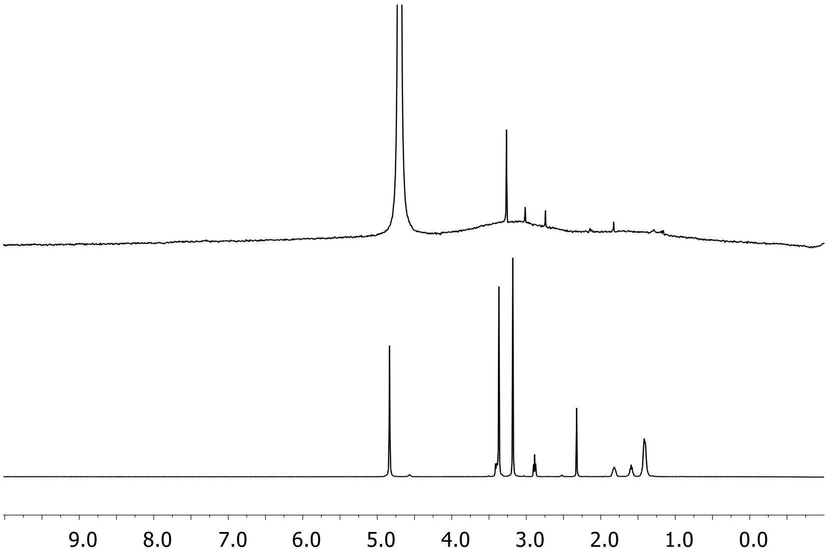

Figure S3: 1H-NMR (500 MHz) spectra of the nanoparticles with 8-trimethylammonium octylthiol in D2O (upper spectrum) and of 8-trimethylammonium octylthioacetate bromide in MeOD (lower spectrum). The upper spectrum reveals only very broad signals in the same chemical shift regions typical of the coating thiol (1.0-2.0 ppm and 2.5-3.5 ppm). Other signal present arise from isotopic impurities of the solvent and traces of other contaminants. This confirms the grafting of the thiol to the nanoparticles (the broadening results from the reduced tumbling rate and mobility of the thiols due to the grafting to the nanoparticles) and their effective purification (no major free organic species are present in the spectrum).

3. Characterization of NP-TPPS hybrids

3.1 TEM analysis of NP-TPPS hybrids

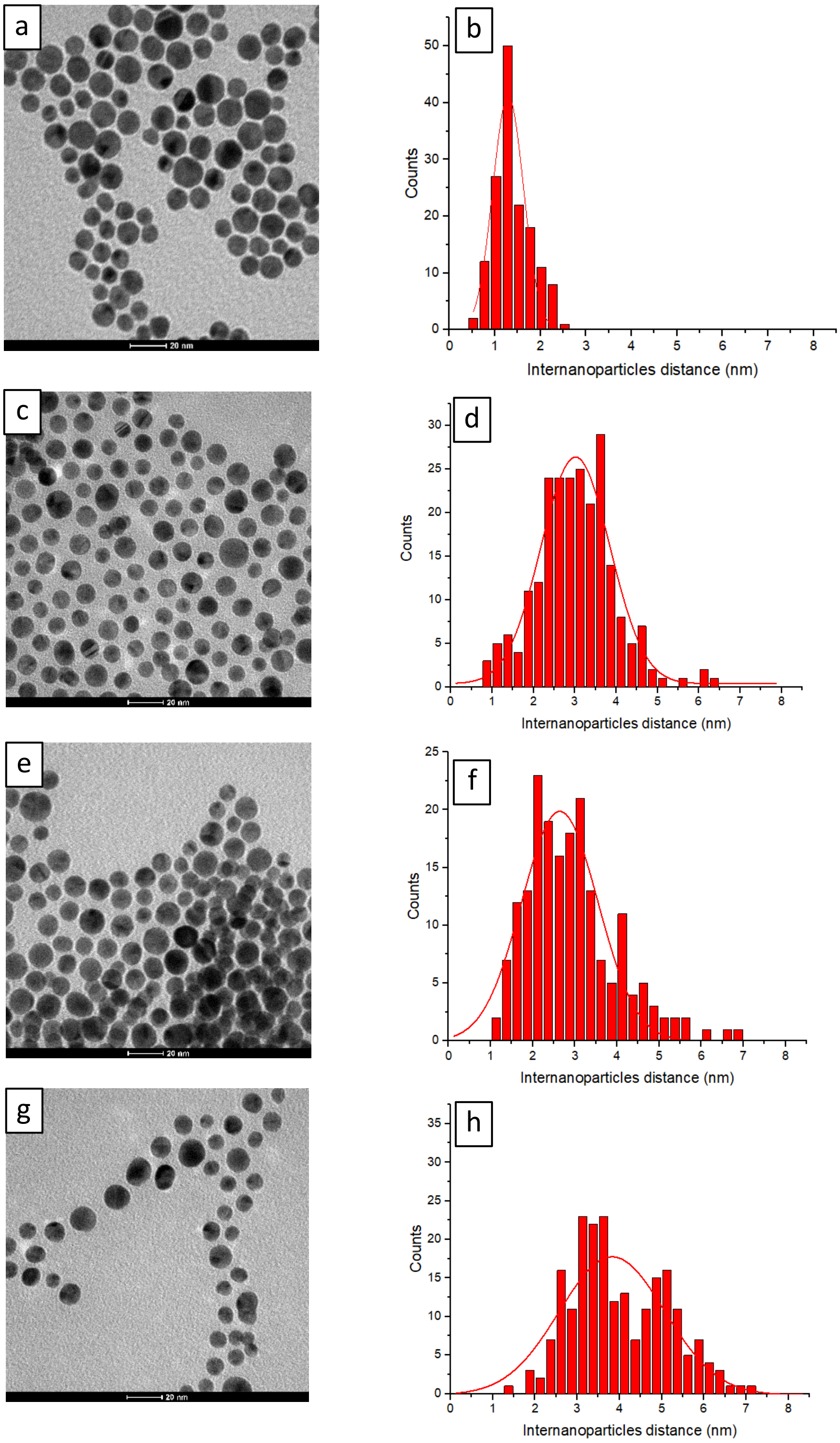

Figure S4: (a, c, e, g) TEM micrographs of nanohybrids at PPP = 0, 100, 1040, 5200, respectively (scale bar: 20 nm); (b, d, f, h) Distribution of the inter-nanoparticle distances of each sample and gaussian fit of the data; (i) most relevant parameters of the fittings of the interparticle distance. Data relative to the NP-TPPS_5200 sample can be fitted also with a bimodal gaussian fit yielding the average interparticle distances of 2.3 and 4.6 nm.

i	Internanoparticles distance (nm)	
PPP	**Centroid**	**FWHM/2**
0	1.3	0.4
100	3.0	1.7
1040	2.7	1.0
5200	3.8	1.4

3.2 Dynamic light scattering measurements

Dynamic Light Scattering (DLS) measures revealed that the hydrodynamic diameter of bare tA-NPs is 12.0 ± 0.8 nm. This figure is in agreement with the average size of the gold core measured with TEM and this implies that tA-NPs, in the absence of porphyrin, are not aggregated. The addition of TPPS molecules resulted in an increased hydrodynamic diameter that goes from 32±8 nm for PPP=100 to 780±60 nm for PPP=1040.

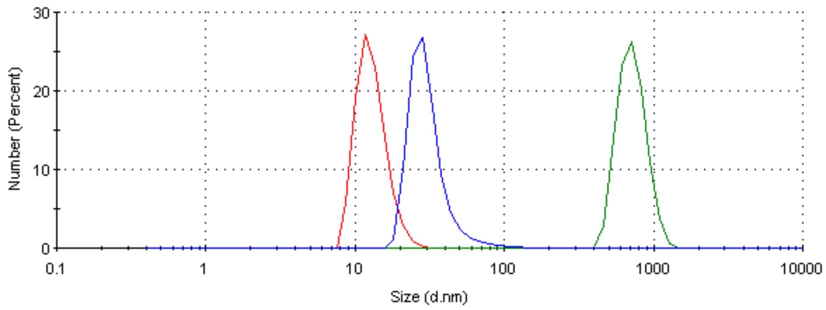

Figure S5: Dynamic Light Scattering (DLS) measurements of bare tA-NPs (PPP=0, red), and NP-TTPS nanohybrids at PPP=100 (blue) and PPP=1040 (green). The hydrodynamic diameter is 12.0 ± 0.8 nm, 32±8 nm and 780±60 nm, respectively.

3.3 Extinction and PL spectra at 77K

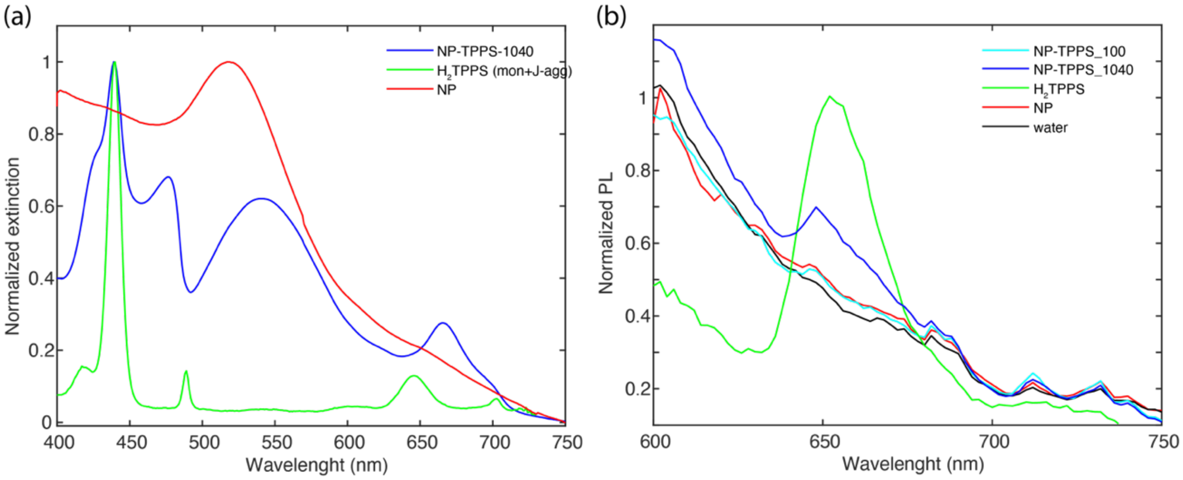

Figure S6. Normalized extinction (a) and PL (b) spectra measured at 77K.

4. Estimation of $E_{\pm}$, δ and $\gamma_{exc,pl}$

Table S1. Summary of the experimental parameters retrieved from the extinction spectra for the calculation of the coupling g for the UR$_Q$/LR$_Q$ and UR$_B$/LR$_B$ resonances (all values in eV). The estimated error is 20%.

	Q	**B**
E_+	2.033	2.605
E_-	1.860	2.175
γ_{exc}	0.052	0.031
γ_{pl}	0.175	0.175
$\Delta E = E_+ - E_-$	0.173	0.43
calculated g	0.11	0.23

5. Simulation of the optical response of gold-NP/J-aggregate nanohybrids

To simulate the absorption spectra of the nanohybrids involving gold NPs and J-aggregates, we consider both materials as continuous dielectric media. We modeled the NP core as a sphere of 11 nm diameter, featuring the dielectric function of gold reported in Ref.[4]. Concentrically to the gold core, we add a spherical shell with a thickness of 1.2 nm, representing the surfactant layer, and we associate it with a dielectric constant of 2.0. Finally, the nanohybrid is built up by attaching two spherical promontories, representing J-aggregates, on diametrically opposite sides of the NP (gold core plus surfactant layer). Such promontory volumes are exterior to the inner sphere (diameter = 11+2.4 nm) and contained within a 9.84 nm diameter sphere centered at its surface (see Scheme S1).

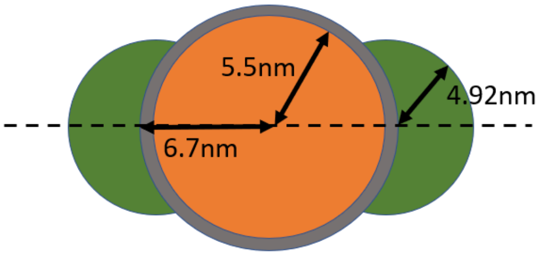

Scheme S1 Arrangement of nanoparticle plus J-aggregate promontories, with indication of sizes.

We estimate the dielectric function of the J-aggregate in the following way. First, we set up the polarizability spectra $\alpha(\omega)$ as a linear combination of two Lorentzian functions. In atomic units,

$$\alpha(\omega) = \frac{2f_Q}{(\omega - i\eta)^2 - \omega_Q^2} + \frac{2f_B}{(\omega - i\eta)^2 - \omega_B^2}$$

where $\omega = h\,c\,/\,\lambda$ is the excitation energy. The B- and Q-band wavelengths are $\lambda_B = 488$ nm and $\lambda_Q = 702$ nm, the B band oscillator strength (assuming it equal to that of the monomer), f_B =1.55 a.u, and the Q/B absorption strengths ratio, f_Q/f_B =0.46. To that aim, data was recovered from our measurements (see the upper panel of Fig. 2 in the main text), the experimental (Ref.[5]) and the theoretical (Ref. [6]) respectively. The factor two in the numerators is due to the degeneracy of the Q and B bands of TPPS, inherited by the J-aggregate. We take $\eta = 0.05$ eV as the linewidth parameter. Second, we supposed a J-aggregate sphere and apply the Clausius-Mossotti relation to find the complex dielectric function $\varepsilon(\omega)$ from the frequency-dependent polarizability. In SI units,

$$\frac{\varepsilon(\omega) - 1}{\varepsilon(\omega) + 2} = \frac{N\alpha(\omega)}{3{n_s}^2\varepsilon_0}$$

where $N = 0.625$ nm^{-3} is the number density of molecules, ε_0 is the vacuum permittivity, $n_s = 1.33$ is the surrounding medium (water) refraction index, and $\alpha(\omega)$ is written in $\mathrm{C}\,m^2/\mathrm{V}$ units. Finally, we arrive at the complex refraction index,

$$n(\omega) = \sqrt{\frac{|\varepsilon(\omega)| + Re\{\varepsilon(\omega)\}}{2}} + i\,\sqrt{\frac{|\varepsilon(\omega)| - Re\{\varepsilon(\omega)\}}{2}}$$

With all the ingredients set, we use the MATLAB toolbox MNPBEM v. 7.0[7] to compute the absorption spectrum of the gold NP (including the surfactant layer), a sphere of J-aggregate (4 nm of diameter), the nanohybrid combining the gold NP and two promontories of J-aggregate (vide supra). For all the systems, we considered the quasi-static approximation. The absorption coefficient reads

$$P_{abs}(\omega) = \frac{4\pi\omega}{c} Im\{d(\omega)\}$$

where $d(\omega)$ is the light-induced dipole moment of the system created by a unitary electric field directed along the promontory-to-promontory axis of the system (dashed line in scheme S1).

For a detailed tutorial of MNPBEM, please see:

http://physik.uni.-graz.at/~uxh/mnpbem/html/mnpbem_gs_top.html.

The results from these procedures lead to the plots in Figure 5 (main text).

6. Simulation of the optical response of linear aggregates of NPs

To show the possible resonance of the monomer Q band with certain arrangements of NPs, we compute the absorption spectrum of necklace-like linear aggregate of 10 NPs with different inter-core distances (0.5 nm, 0.7 nm and 1 nm). The aggregate with the inter-core distance of 0.7 nm is the closest to the aforementioned resonance, as shown in Figure S6 (below). Note that by "inter-core distance" we mean the distance between the surface of the gold cores in nearby NPs. To achieve such distances, the surfactant shells should partly interpenetrate. We built up the overall surfactant layer of the full system by interlocking 10 spherical shells. Each of the former is placed concentrically and outside each of the NP's core, and it is 1.2 nm thick.

To compute the reference absorption spectrum of the monomer, we proceed analogously as in the previous section for the J-aggregate. That is, we set up a polarizability function which is a linear combination of two Lorentzians associated with the monomer B and Q bands. The corresponding wavelengths ($\lambda_B = 435$ nm and $\lambda_Q = 645$ nm) are taken from our experiment (see Fig. 2, main text), as the absorption strength ratio (f_Q/f_B =0.1). To find the complex dielectric function from Clausius Mossotti equation, we use a number density of molecules of $N = 0.1$ nm^{-3}**.** The rest of the parameters are the same as for the J-aggregate case.

Finally, we use MNPBEM[7] to compute quasi-static absorption spectrum of the 10 NP linear aggregate (including the surfactant layer) and a sphere of TPPS (4 nm of diameter). Note that the maximum size of the largest system considered (~120 nm) is still smaller than the absorption wavelengths, so using the quasi-static approach, although approximated, is still reasonable.[7]

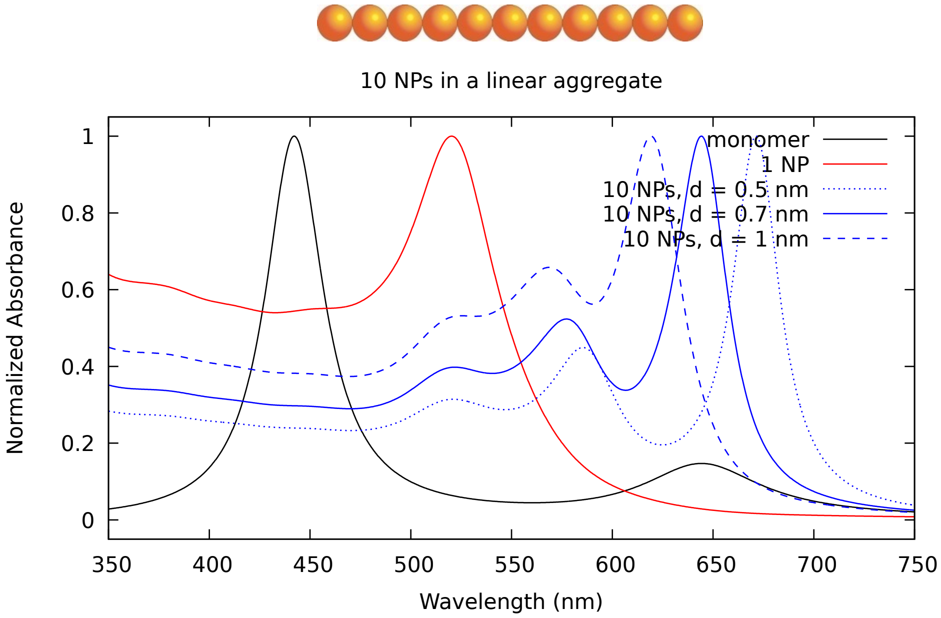

Figure S7. Simulated normalized absorption spectrum for a H_2-TPPS^{2-} monomer (black), a capped gold NP (red), and a 10 NPs necklace-like aggregate (cartoon on top) at different inter-particle distance (blue).

References

1 R. Bonomi, A. Cazzolaro and L. J. Prins, *Chem. Commun.*, 2011, **47**, 445–447.

2 H. Xia, S. Bai, J. Hartmann and D. Wang, *Langmuir*, 2010, **26**, 3585–3589.

3 V. Amendola, R. Pilot, M. Frasconi, O. M. Maragò and M. A. Iatì, *J. Phys. Condens. Matter*, 2017, **29**, 203002.

4 P. B. Johnson and R. W. Christy, *Phys. Rev. B*, 1972, **6**, 4370–4379.

5 E. . Tokunaga and K. Nakata, in *J-Aggregates, Volume 2*, ed. T. Kobayashi, World Scientific, Singapore, 2012, pp. 213–246.

6 R. Improta, C. Ferrante, R. Bozio and V. Barone, *Phys. Chem. Chem. Phys.*, 2009, **11**, 4664–4673.

7 U. Hohenester and A. Trügler, *Comput. Phys. Commun.*, 2012, **183**, 370–381.